Journal of Solid State Chemistry 183 (2010) 2968–2973

Contents lists available at ScienceDirect

Journal of Solid State Chemistry

journal homepage: www.elsevier.com/locate/jssc

Synthesis of Fe_3O_4\SiO_2\Ag nanoparticles and its application in surface-enhanced Raman scattering

Baoliang Lv, Yao Xu *, Hong Tian, Dong Wu, Yuhan Sun

State Key Laboratory of Coal Conversion, Institute of Coal Chemistry, Chinese Academy of Sciences, Taiyuan 030001, China

ARTICLE INFO

Article history:
Received 16 April 2010
Received in revised form
26 September 2010
Accepted 3 October 2010
Available online 16 October 2010

Keywords:
Ultrasonic synthesis
Fe_3O_4\SiO_2\Ag
Core\shell\particle
SERS

ABSTRACT

To obtain a recyclable surface-enhanced Raman scattering (SERS) material, we developed a composite of Fe_3O_4\$SiO_2$\Ag with core\shell\particles structure. The designed particles were synthesized via an ultrasonic route. The Raman scattering signal of Fe_3O_4 could be shielded by increasing the thickness of the SiO_2 layer to 60 nm. Dye rhodamine B (RB) was chosen as probe molecule to test the SERS effect of the synthesized Fe_3O_4\$SiO_2$\Ag particles. On the synthesized Fe_3O_4\$SiO_2$\Ag particles, the characteristic Raman bands of RB could be observed when the RB solution was diluted to 5 ppm (1×10^{-5} M). Furthermore, the synthesized particles could keep their efficiency till four cycles.

1. Introduction

Since the first report on surface-enhanced Raman scattering (SERS) phenomena was found in silver and gold sols in 1979 [1], many researches were focused on this attractive field because of its wide applications in the study of sensors, catalysis, molecule structures, adsorption of molecules, coordination chemistry, drug\nucleic acid interactions and so on [2,3]. In the past decades, most of the correlative SERS studies mainly focused on four goals. (i) Develop and improve the SERS substrates. Studies focused on this goal remained an active area of research and many publications were devoted to the descriptions of novel substrates as well as to the investigations of more conventional substrates. Producing inexpensive SERS materials of rugged and sensitive surfaces for analytical applications was the goal of the most SERS substrate development work at all times [4–6]. (ii) Increase the sensitivity of the SERS substrate. Actually, SERS analysis has achieved a single molecule level by Kneipp and his group [7] as early as 1997, but many improvements are still in progress until now [8,9]. (iii) Study the relative basic theory of SERS. The study of SERS theory has always been an active research area since the SERS effect was discovered, and many publications were still devoted to this field in recent years [10,11]. (iv) Explore the new applications of SERS. Up to now, SERS phenomenon has been applied in many fields as mentioned at the beginning of this paragraph and new applications are still continuously developed [12–14]. It is interesting to note that, in most of these works, noble metal colloids or particles with nanostructures (including Au, Ag, Pt, Pd, Ru and their composites) [15–20] were the most commonly used SERS substrates. However, the use of noble metals directly increased the cost of SERS detection. To resolve this problem, there are two methods: (i) Seeking for cheap materials with SERS effect, which can substitute noble metals. Many researches were carried out for this purpose, but most of these materials exhibited poor SERS effect in comparison with the noble metals (for instance Cu [21], Cu–Zr alloys [22], α-Fe_2O_3 [6], porous silicon [23] and so on). (ii) Exploiting recyclable SERS materials based on noble metals. However, reports on callback and recycle of SERS materials were very few [24,25].

Out of this consideration, we planned to prepare a recyclable SERS material, Fe_3O_4\Ag particles of core\shell structure, on the basis of SERS material Ag nanoparticles and magnetic Fe_3O_4 nanoparticles. However, Fe_3O_4 has obvious Raman scattering at 665 and 540 cm^{-1} [26], and its scattering would be further enhanced after coating with Ag nanoparticles due to the SERS effect. According to the literatures [27,28], amorphous SiO_2 have no Raman scattering. Therefore, a SiO_2 layer was inserted between Fe_3O_4 core and Ag particles to shield the Raman scattering of Fe_3O_4. Actually, there have been many reports on the preparation of Fe_3O_4\$SiO_2$ and SiO_2\Ag nanoparticles [29–31]. However, the synthesis of Fe_3O_4\$SiO_2$\Ag particles is still not reported until now. Herein, we prepared the Fe_3O_4\$SiO_2$\Ag particles via a simple and effective ultrasonic route, and studied its possible application in SERS.

2. Experimental section

2.1. Synthesis of Fe_3O_4 nanoparticles

The Fe_3O_4 nanoparticles were obtained by a polyol reducing process in a solvothermal system. In a typical procedure, 2.70 g of

* Corresponding author. Fax: +86 351 4041153.
E-mail address: xuyao@sxicc.ac.cn (Y. Xu).

0022-4596/$ - see front matter © 2010 Elsevier Inc. All rights reserved.
doi:10.1016/j.jssc.2010.10.001

$FeCl_3 \cdot 6H_2O$ and 4.10 g of $NaAc \cdot 3H_2O$ (as a dispersed agent) were added to 80 mL of ethylene glycol (EG), which acted as both solvent and reductant. The solution was then sealed in a 100 mL Teflon-lined stainless steel autoclave and treated for 24 h at 180 °C. At last, black precipitate was obtained at the bottom of the autoclave and separated by magnetic force. After that, the precipitate was washed three times with ethanol and dried at 60 °C in air.

2.2. Preparation of Fe_3O_4\SiO_2 particles

Fe_3O_4\SiO_2 structures were prepared by an assisted Stöber process. A total of 0.05 g of synthesized Fe_3O_4 nanoparticles were re-dispersed in solution composed of 100 mL of ethanol and 10 mL of $NH_3 \cdot H_2O$. Then, 0.02 mL of TEOS was added to the solution and the solution was ultrasonicated for 2 h using an ultrasonic cleaning bath. After that, the precipitate was separated by magnetic force and washed three times with ethanol. The thickness of the SiO_2 layer could be adjusted by changing the cycle times of the coating process.

2.3. Preparation of Fe_3O_4\SiO_2\Ag particles

To locate Ag nanoparticles on the surface of Fe_3O_4\$SiO_2$, an electroless metal plating process was carried out [30]. The new synthesized Fe_3O_4\$SiO_2$ particles were dispersed in 50 mL mixture solution of $SnCl_2$ (0.60 g) and HCl (0.01 M) and the solution was ultrasonicated for 30 min. Subsequently, the particles were separated by magnetic force and quickly washed three times with distilled water. Then, the particles were re-dispersed in 50 mL of fresh aqueous solution of ammonical silver nitrate (0.13 M) and sonicated for 1 h. At last, the precipitate was separated by magnetic force, washed three times with distilled water and then dried at 60 °C in air.

2.4. Instruments

X-ray diffraction (XRD) measurement was performed on a D8 Advance Bruker AXS diffractometer using Cu–$K\alpha$ radiation (λ=1.5406 Å). The morphologies of the samples were observed by transmission electron micrograph (TEM, Hitachi H-600 and JEM-2010). X-ray photoelectron spectroscopy (XPS) analysis was performed on a PHI 5300x multi-technique system with an Mg $K\alpha$ X-ray source (Perkin-Elmer Physical Electronics). Raman spectra were measured on a Horiba Labram HR800 spectrometer equipped with 514 nm argon ion laser.

3. Results and discussion

Fig. 1 shows the XRD patterns of the products at different steps: (a) Fe_3O_4 particles, (b) Fe_3O_4\$SiO_2$ particles and (c) Fe_3O_4\$SiO_2$\Ag particles. From Fig. 1a, the initial synthesized product can be indexed to Fe_3O_4 according to standard data (JCPDS 19-0629). After being coated by SiO_2, the intensity of the Fe_3O_4 phase decreased obviously and a wide diffraction of amorphous SiO_2 could be found between 20° and 30° of 2θ, as shown in Fig. 1b. Fig. 1c shows the patterns of Fe_3O_4\$SiO_2$\Ag particles, in which the (1 1 1) peak of Ag (JCPDS 04-0783) could be found clearly at 38° of 2θ.

The morphologies and structures of the products at different synthetic steps were observed by TEM. Fig. 2a shows the TEM image of Fe_3O_4 particles, in which well-dispersed particles with average diameter about 150 nm could be observed clearly. Seen from the TEM image of Fe_3O_4\$SiO_2$ particles (Fig. 2b), the core\shell structure could be clearly observed and the thickness of the SiO_2 layer is about 60 nm. The TEM image of the Fe_3O_4\$SiO_2$\Ag particles is shown in Fig. 2c, in which small nanoparticles are uniformly

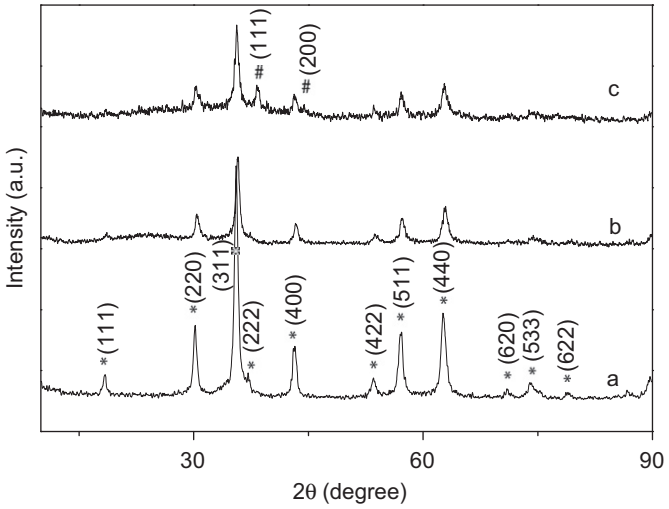

Fig. 1. XRD patterns of products at different step: (a) Fe_3O_4, (b) Fe_3O_4\$SiO_2$ and (c) Fe_3O_4\$SiO_2$\Ag. (#: Ag 04-0783, and ∗: Fe_3O_4 19-0629).

distributed on the surface Fe_3O_4\$SiO_2$ particles. To identify the situation of Ag element, HRTEM was used to observe the detailed information of the synthesized particles. Fig. 2d is an image of a single particle with core\shell\Ag structure, and Fig. 2e is the high-magnification image of the E area in Fig. 2d. It is seen from Fig. 2e that there are many isolated little crystal areas (the oval areas in Fig. 2e) on the shell of the particle. Fig. 2f is a typical image of the crystal area (F area in Fig. 2e), in which two kinds of lattice fringes can be readily resolved and the inter-plane distances are both 0.29 nm that is very close to the inter-plane distances of (1-10) and (0-11) planes of Ag (JCPDS 04-0783). According to the corresponding fast-Fourier transform (FFT, inset of Fig.2f) analysis, the image should be the projection of (111) planes under incident electron beam along [111] direction of Ag. On the basis of above analysis, the core\shell\particle structure of Fe_3O_4\$SiO_2$\Ag particles could be identified and the Ag particles are well distributed on the surface Fe_3O_4\$SiO_2$ particles.

Fig. 3 shows the XPS spectrum of the synthesized Fe_3O_4\$SiO_2$\Ag particles. Seen from the high-resolution spectrum (inset of Fig. 3) between 730 and 700 eV, the typical peaks of Fe element at the binding energies of 724.5 eV (Fe 2p1/2) and 711.0 eV (Fe 2p3/2) are not found, and the peak at 716.3 eV should be the peak of Sn 3p3 [30,32]. This indicates that the Fe_3O_4 particles have been coated completely, since the analysis depth of XPS is only several nanometers. Both the peaks of Si 2s (153.5 eV) and Si 2p (102.6 eV) are very small and this means that SiO_2 is not the main component of the outer surface. The strong peaks of Ag 3p1 (603.5 eV), Ag 3p3 (573.2 eV), Ag 3d5/2 (368.2 ev) and Ag 3d7/2 (374.3 ev) indicate that Ag is the main component of the surface, and these peaks also demonstrate that the Ag element in the sample is Ag^0 [32,33]. The peaks of Sn 3d and Sn 3p should come from the adsorbed Sn^{4+} or Sn^{2+}. On the basis of above analysis, it can be concluded that the XPS data further identified the core\shell\particles structure of the synthesized Fe_3O_4\$SiO_2$\Ag particles.

In the preparation process, one very important step was to load the Ag nanoparticles on the SiO_2 surface of Fe_3O_4\SiO_2 particles. In order to obtain uniform silver nanoparticles and their effective bonding with silica surface, the pre-treatment process used in electroless plating method was adopted [30]. It is a widely used process in electroless plating to deposit some metal nanoparticles such as gold and palladium on the surface of a substrate as a catalyst [34]. In this method, the ions used as reductant were firstly adsorbed on the surface of the substrate, which were subsequently dispersed in the solution of aimed metal ions. Then, reaction would

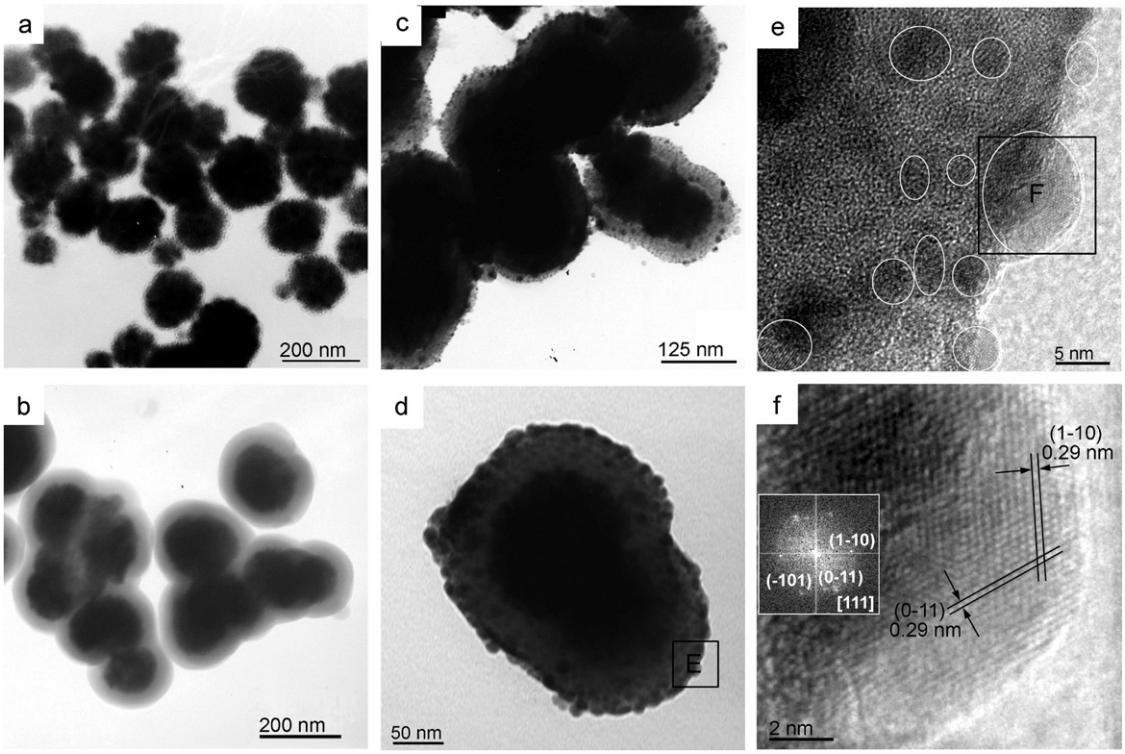

Fig. 2. TEM images of (a) Fe_3O_4, (b) Fe_3O_4\$SiO_2$, (c) and (d) Fe_3O_4\$SiO_2$\Ag, (e) the E area in (d), (f) the F area in (e) (ellipses in (e) are crystal areas, and inset of (f) is its corresponding FFT image).

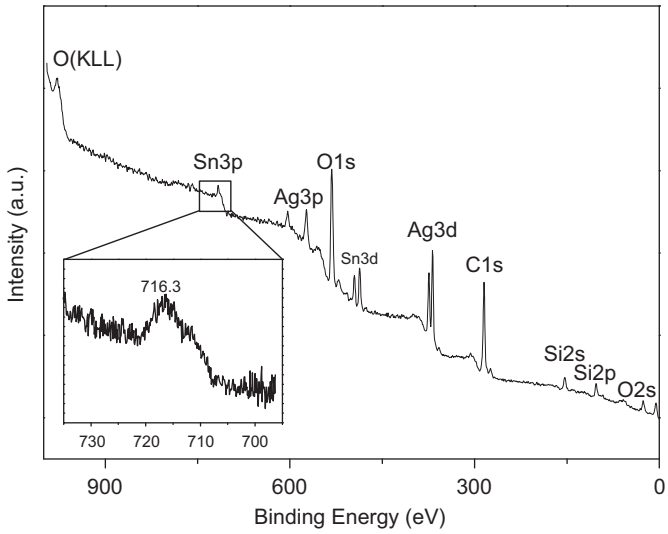

Fig. 3. XPS spectrum of Fe_3O_4\SiO_2\Ag particles and the inset is the high-resolution spectrum of 730–700 eV.

uniformly occur on the surface of substrate and the nuclei of aimed metal would also be uniformly formed on the surface. Subsequently, the metal nanoparticles would uniformly grow on the surface of the substrate. As the nuclei were directly formed on the hetero matrix–metal interface, the formed bonding between metal nuclei and matrix obtained by hetero-interface nuclei formation would be superior to homogeneous nuclei process in the solution. In the homogeneous nuclei process, silver nuclei were formed in the solution where most of the as-formed silver nuclei suspend, and small part of silver nuclei moves to the silica surface to form a loose bonding through adsorption effect. In our synthesis process, Sn^{2+} ions were selected as the reductant to load Ag nanoparticles on the Fe_3O_4\SiO_2 particles, because the Sn^{2+} ions not only could reduce the Ag^+ to Ag^0, but also could easily adsorb on the surface of SiO_2 through interaction with the surface hydroxyl groups and the electrostatic interaction with the negatively charged surface [30,34]. The adsorption of reducing agent Sn^{2+} ions firstly took place on the silica surface. Then, when the $Ag[(NH_3)_2]^+$ ions were added into the solution, the following reaction would occur

$$Sn^{2+} + 2[Ag(NH_3)_2]^+ \rightarrow Sn^{4+} + 2Ag + 2NH_3$$

By this way, the silver nanoparticles were uniformly formed on the hetero silica–silver interface and possessed good stability. The whole process is illustrated in Sketch 1.

As mentioned in the introduction, the SiO_2 layer was inserted between the Fe_3O_4 core and the Ag particles to shield the Raman scattering of Fe_3O_4. However, the magnetic response capability of the ultimate product might be weakened if the SiO_2 layer was too thick. Therefore, taking into account the magnetic response capability and the Raman scattering of Fe_3O_4, the confirmation of the appropriate thickness of SiO_2 layer became a question. To resolve this problem, Fe_3O_4\$SiO_2$ particles with different SiO_2 layer in thickness were synthesized by changing the repeat times of the coating process. Fig. 4 shows the TEM images of the Fe_3O_4\$SiO_2$ particles with different SiO_2 layer. The thickness of SiO_2 layers in Figs. 4a–c is 15, 40 and 60 nm, respectively. Fig. 4d shows the photograph of Fe_3O_4\$SiO_2$ particles with 60 nm SiO_2 layer before and after it was placed in a magnetic field for 30 s, in which the synthesized Fe_3O_4\$SiO_2$ particles could be separated out of solution easily. That is to say, the Fe_3O_4\$SiO_2$ particles showed good magnetic response ability even if the SiO_2 layer was increased to 60 nm. Then, Ag nanoparticles were loaded on the surfaces of these Fe_3O_4\$SiO_2$ particles with different SiO_2 layer. Subsequently, Raman analysis was carried out on these different Fe_3O_4\$SiO_2$\Ag particles,

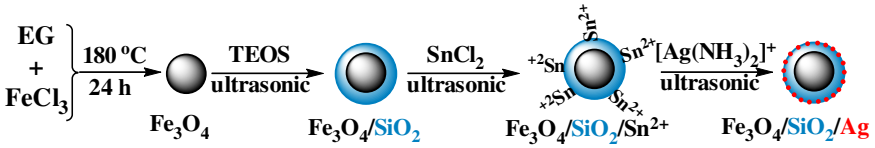

Sketch 1.

Sketch 1. Illustration of the ultrasonic synthesis route of Fe_3O_4\SiO_2\Ag particles.

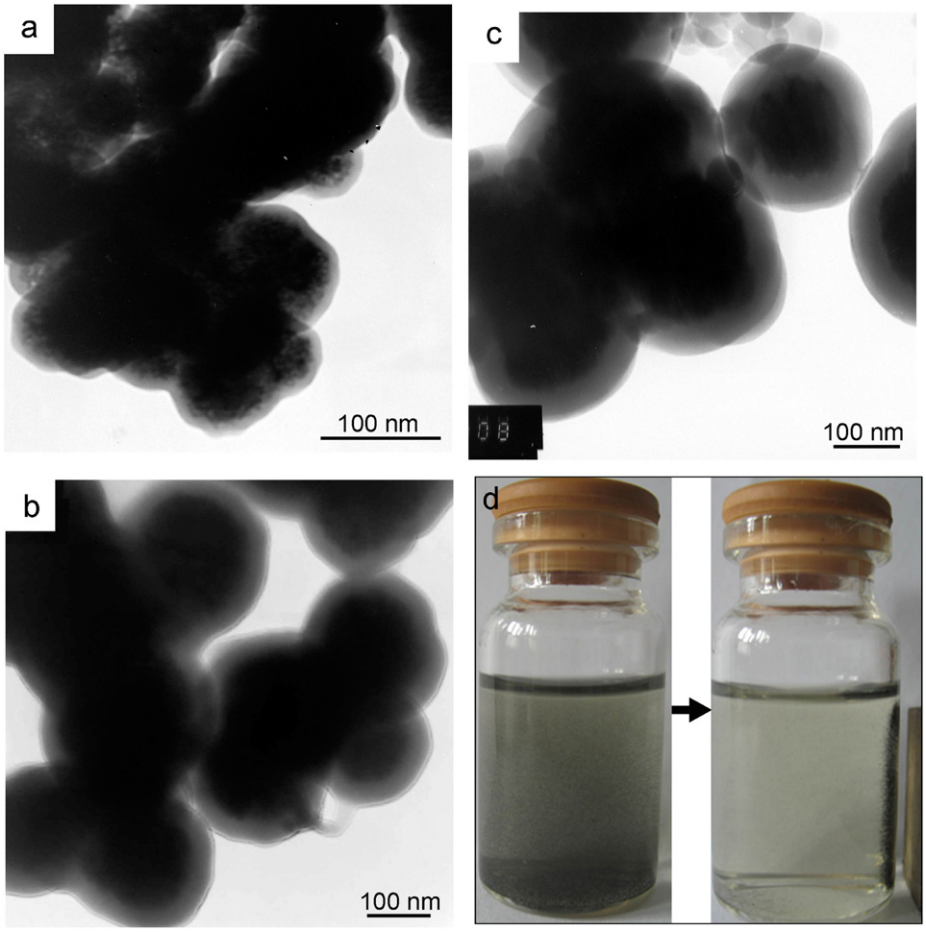

Fig. 4. Fe_3O_4\SiO_2 particles with different SiO_2 layer in thickness: (a) 15 nm, (b) 40 nm and (c) 60 nm; (d) is the photograph of before and after the sample (c) was placed in a magnetic field for 30 s.

and their spectra are shown in Fig. 5A. It is notable that the Raman scattering of α-Fe_2O_3 and γ-Fe_2O_3 also could be found in Fig.5A (a), which should be attributed to the surface oxidization of Fe_3O_4 particles in the SiO_2 coating process. It was found that the intensity of the Raman scattering of the iron oxides decreased with the increase in thickness of the SiO_2 layer. When the thickness of SiO_2 layer was increased to 60 nm, the Raman scattering of iron oxides could be shielded completely.

Dye rhodamine B (RB) was chosen as the probe molecule to test the SERS effect of the synthesized Fe_3O_4\$SiO_2$\Ag particles. Fig. 5B (a) shows the Raman spectra of pure RB, in which the bands at 1198, 1357, 1505, 1560 and 1649 cm^{-1} could be confirmed as its characteristic bands. Fig. 5B (b) shows the Raman spectra of RB solution (40 ppm, 8×10^{-5} M) on a SiO_2 nanoparticles substrate, seen from which there was no characteristic bands of RB could be observed. Fig. 5B (c) shows the Raman spectra of the same RB solution on the synthesized Fe_3O_4\$SiO_2$\Ag particles substrate, in which the characteristic bands of RB at 1198, 1357, 1505, 1560 and 1649 cm^{-1} could be found clearly. That is to say, the synthesized Fe_3O_4\$SiO_2$\Ag particles had obvious SERS effect. To investigate the SERS sensitivity of the Fe_3O_4\$SiO_2$\Ag particles, the RB solution was diluted to 20 (4×10^{-5} M), 10 (2×10^{-5} M), 5 ppm (1×10^{-5} M), and their Raman spectra on the synthesized Fe_3O_4\$SiO_2$\Ag particles are shown in Fig. 5B (d)–(f), respectively. It was found that the intensity of the characteristic bands of RB decreased with the decrease of the RB concentration, and the characteristic bands still could be found even when the solution was diluted to 5 ppm, though the signal intensity was not very strong.

To test the recycling performance of the synthesized Fe_3O_4\'" SiO_2\Ag particles, the used sample was ultrasonically washed three times with water and ethanol, respectively. After that, the sample was detected and its Raman spectra are shown in Fig. 5C (a), in which no bands could be observed. Then, the recycling performance of Fe_3O_4\SiO_2\Ag particles was investigated with RB

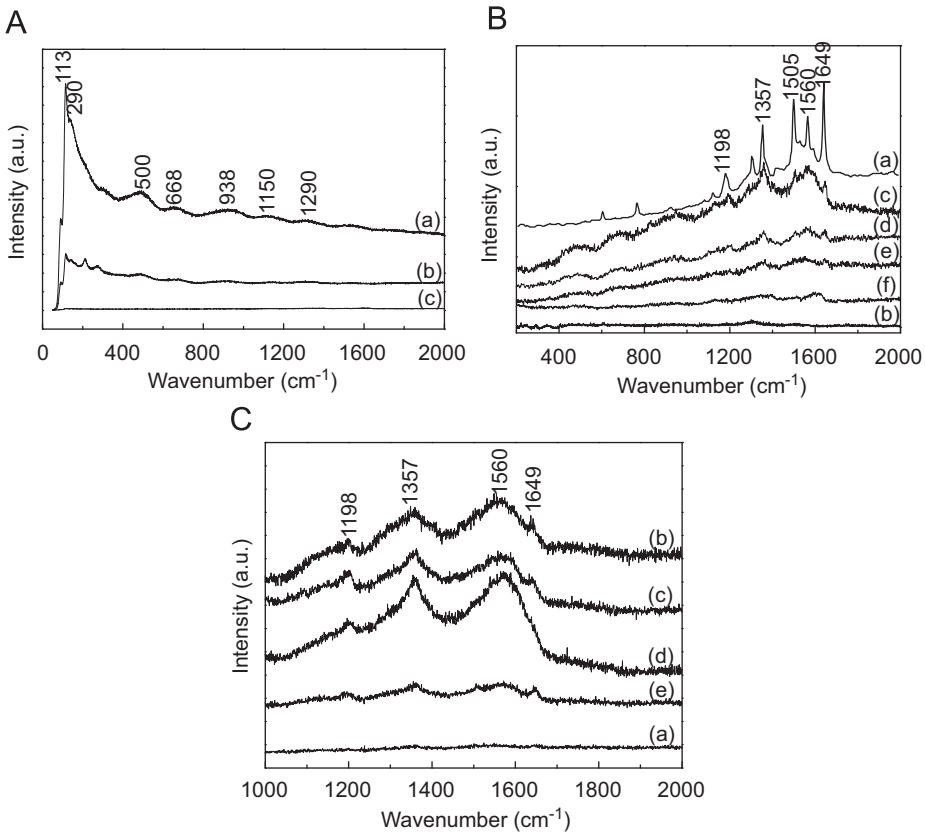

Fig. 5. (A) Raman spectra of $Fe_3O_4\backslash SiO_2\backslash Ag$ particles with different SiO_2 layer in thickness: (a) 15 nm, (b) 40 nm and (c) 60 nm; (B) Raman spectra of (a) pure dye RB, (b) RB solution (40 ppm, 8×10^{-5} M) on SiO_2 particles, RB solutions with different concentration on synthesized $Fe_3O_4\backslash SiO_2\backslash Ag$ particles (c) 40 ppm, (d) 20 ppm, (e) 10 ppm and (f) 5 ppm; (C) (a) Raman spectra of the ultrasonically washed $Fe_3O_4\backslash SiO_2\backslash Ag$ particles after first cycle; Raman spectra of RB solution (40 ppm, 8×10^{-5} M) to test the recycling performance of the synthesized $Fe_3O_4\backslash SiO_2\backslash Ag$ particles: (b) second cycle, (c) third cycle, (d) fourth cycle and (e) fifth cycle.

solution (40 ppm, 8×10^{-5} M). It was found that the synthesized particles exhibited good stability and recycling performance in the second, third and fourth cycle, as shown in Fig. 5C (b)–(d), respectively. In the fifth cycle, the efficiency decreased slightly (Fig. 5C (e)) that should be owing to the loss of the silver nanoparticles. In next step, we plan to make a thin SiO_2 coating (about 10 nm) for the whole particle and form a $Fe_3O_4\backslash SiO_2\backslash Ag\backslash SiO_2$ structure to avoid the loss of the silver particles. The correlative experiments are on progress now.

4. Conclusions

In summary, $Fe_3O_4\backslash SiO_2\backslash Ag$ particles were synthesized via a simple ultrasonic route. The Raman scattering of Fe_3O_4 could be shielded by increasing the thickness of the SiO_2 layer to 60 nm. The synthesized $Fe_3O_4\backslash SiO_2\backslash Ag$ particles exhibited good sensitivity, stability and well-recycling performance in SERS. Although it has a distance to the single molecule level SERS, the synthesized particles still testified the feasibility of developing recyclable SERS materials. The stability and recycling performance of this material may be further improved by increasing a thin SiO_2 layer on $Fe_3O_4\backslash SiO_2\backslash Ag$ particles and that is the next aim of our work.

References

[1] J.A. Creighton, C.G. Blatchford, M.G. Albretch, J. Chem. Soc. Faraday Trans. II 75 (1979) 790–798.
[2] R.F. Aroca, R.A. Alvarez-Puebla, N. Pieczonka, S. Sanchez-Cortez, J.V. Garcia-Ramos, Adv. Colloid Interface Sci. 116 (2005) 45–61.
[3] L.A. Lyon, C.D. Keating, A.P. Fox, B.E. Baker, L. He, S.R. Nicewarner, S.P. Mulvaney, M.J. Natan, Anal. Chem. 70 (1998) 341–362.
[4] P. Nielsen, S. Hassing, O. Albrektsen, S. Foghmoes, P. Morgen, J. Phys. Chem. C 113 (2009) 14165–14171.
[5] G.B. Braun, S.J. Lee, T. Laurence, N. Fera, L. Fabris, G.C. Bazan, M. Moskovits, N.O. Reich, J. Phys. Chem. C 113 (2009) 13622–13629.
[6] X. Fu, F. Bei, X. Wang, X. Yang, L. Lu, Mater. Lett. 63 (2009) 185–187.
[7] K. Kneipp, Y. Wang, H. Kneipp, L.T. Perelman, I. Itzkan, R.R. Dasari, M.S. Feld, Phys. Rev. Lett. 78 (1997) 1667–1670.
[8] M. Futamata, Y. Maruyama, M. Ishikawa, J. Mol. Struct. 735–736 (2005) 75–84.
[9] B. Vlckova, I. Pavel, M. Sladkova, K. Siskova, M. Slouf, J. Mol. Struct. 834-836 (2007) 42–47.
[10] V.N. Pustovit, T.V. Shahbazyan, Chem. Phys. Lett. 420 (2006) 469–473.
[11] A. Otto, A. Bruckbauer, Y.X. Chen, J. Mol. Struct. 661-662 (2003) 501–514.
[12] K. Cottingham, Anal. Chem. 81 (2009) 7128.
[13] I. Delfino, A.R. Bizzarri, S. Cannistraro, Biophys. Chem. 113 (2005) 41–51.
[14] S. Efrima, L. Zeiri, J. Raman Spectrosc. 40 (2009) 277–288.
[15] D. Philip, K.G. Gopchandran, C. Unni, K.M. Nissamudeen, Spectrochim. Acta Part A 70 (2008) 780–784.
[16] D. Philip, Spectrochim. Acta Part A 71 (2008) 80–85.
[17] B. Ren, X.F. Lin, Z.L. Yang, G.K. Liu, R.F. Aroca, B.W. Mao, Z.Q. Tian, J. Am. Chem. Soc. 125 (2003) 9598–9599.
[18] Y. Yang, S. Matsubara, L. Xiong, T. Hayakawa, M. Nogami, J. Phys. Chem. C 111 (2007) 9095–9104.
[19] J. Solla-Gullón, R. Gómez, A. Aldaz, J.M. Pérez, Electrochem. Commun. 10 (2008) 319–322.
[20] J.W. Hu, Y. Zhang, J.F. Li, Z. Liu, B. Ren, S.G. Sun, Z.Q. Tian, T. Lian, Chem. Phys. Lett. 408 (2005) 354–359.
[21] B. Bozzini, C. Mele, E. Tondo, Electrochim. Acta 55 (2010) 3279–3285.
[22] A. Kudelski, J. Bukowska, M. Dolata, W. Grochala, A. Szummer, M. Janik-Czachor, Mater. Sci. Eng. A 267 (1999) 235–239.
[23] A.Y. Panarin, S.N. Terekhov, K.I. Kholostov, V.P. Bondarenko, Appl. Surf. Sci. 256 (2010) 6969–6976.
[24] P. Aldeanueva-Potel, E. Faoucher, R.A. Alvarez-Puebla, L.M. Liz-Marzán, M. Brust, Anal. Chem. 81 (2009) 9233–9238.
[25] X. Li, G. Chen, L. Yang, Z. Jin, J. Liu, Adv. Funct. Mater. 20 (2010) 2815–2824.
[26] O.N. Shebanova, P. Lazor, J. Raman Spectrosc. 34 (2003) 845–852.
[27] F.X. Liu, Y. Xiao, Y.S. Li, J. Raman Spectrosc. 32 (2001) 73–77.
[28] K. Kim, H.S. Kim, H.K. Park, Langmuir 22 (2006) 8083–8088.

[29] A.L. Morel, S.I. Nikitenko, K. Gionnet, A. Wattiaux, J. Lai-Kee-Him, C. Labrugere, B. Chevalier, G. Deleris, C. Petibois, A. Brisson, M. Simonoff, ACS Nano 2 (2008) 847–856.
[30] Y. Kobayashi, V. Salgueiriño-Maceira, L.M. Liz-Marzán, Chem. Mater. 13 (2001) 1630–1633.
[31] H. Li, C.S. Ha, I. Kim, Nanoscale Res. Lett. 4 (2009) 1384–1388.
[32] J.F. Moulder, W.F. Stickle, P.E. Sobol, K.D. Bomben, Handbook of X-Ray Photoelectron Spectroscopy, Physical Electronics, Perkin-Elmer Eden Prairie, American, Minnesota, 1995.
[33] I. Lopez-Salido, D.C. Lim, Y.D. Kim, Surf. Sci. 588 (2005) 6–18.
[34] G.O. Mallory, J.B. Hajdu, Electroless Plating: Fundamentals and Applications, American, Orlando, 1990.